The role of inward Na^+–Ca^{2+} exchange current in the ferret ventricular action potential

N. C. Janvier, S. M. Harrison and M. R. Boyett*

Department of Physiology, University of Leeds, Leeds LS2 9JT, UK

1. Inward Na^+–Ca^{2+} exchange current (i_{NaCa}) was either blocked in ferret ventricular cells by replacing extracellular Na^+ with Li^+ or substantially reduced by the almost complete elimination of the Ca^{2+} transient by buffering intracellular Ca^{2+} with the acetoxymethyl ester form of BAPTA (BAPTA AM).

2. During square wave voltage clamp pulses to 0 mV, replacing extracellular Na^+ with Li^+ or buffering intracellular Ca^{2+} with BAPTA AM resulted in the loss of a transient inward current. This current was increased by the application of isoprenaline (expected to increase the underlying Ca^{2+} transient) and displayed the voltage-dependent characteristics of inward i_{NaCa}.

3. Replacing extracellular Na^+ with Li^+ or buffering intracellular Ca^{2+} caused a significant shortening of the action potential (at −65 mV, $44 \pm 2\%$ with Li^+ and $20 \pm 2\%$ with BAPTA AM). The shortening can be explained by changes in i_{NaCa}.

4. The action potential clamp technique was used to measure the BAPTA-sensitive current (putative i_{NaCa}) and the Ca^{2+} current (i_{Ca}; measured using nifedipine) during the action potential. Under control conditions, the inward BAPTA-sensitive current makes approximately the same contribution as i_{Ca} during much of the action potential plateau. These results suggest an important role for inward i_{NaCa} in the ferret ventricular action potential.

In atrial and rat ventricular cells it is well established that the low plateau of the action potential, which occurs at relatively negative potentials, is generated by inward Na^+–Ca^{2+} exchange current (i_{NaCa}) activated by the Ca^{2+} transient (Mitchell, Powell, Terrar & Twist, 1984; Noble, Noble, Bett, Earm, Ho & So, 1991; Janvier & Boyett, 1996*a*). The ventricular action potential of most species, however, displays a high broad plateau at more positive potentials (+60 to −20 mV) during which the role of i_{NaCa} is unclear. Unlike the case in atrial cells, the peak of the Ca^{2+} transient in ventricular cells occurs at positive potentials at which the driving force for inward i_{NaCa} is small. Consequently the inward current is expected to be relatively small compared with its magnitude in the low plateau in atrial cells. Furthermore, other currents, principally the Ca^{2+} current (i_{Ca}), are thought to contribute significantly to the ventricular plateau and unlike the case in atrial cells there is no clear separation of i_{Ca} and i_{NaCa} during the action potential to help the investigator determine their relative roles (Noble *et al.* 1991). Nevertheless, Mitchell *et al.* (1984) suggested that an inward current activated by intracellular Ca^{2+} (possibly i_{NaCa}) contributes to the plateau in guinea-pig ventricular cells, because buffering of intracellular Ca^{2+} shortened the action potential.

Specific inhibition of the Na^+–Ca^{2+} exchanger is impractical for understanding the role of the current in the action potential. Intracellular application of the exchanger inhibitory peptide (XIP) in rat ventricular cells caused the rapid appearance of spontaneous contractile waves (Bouchard, Clark & Giles, 1993), presumably due to Ca^{2+} overload, making any interpretation of the results highly complex. A more successful approach to the problem has been the use of 'tail currents' to measure inward i_{NaCa}. Interruption of action potentials by clamping a cell to potentials negative to −40 mV elicits slowly decaying currents that have been attributed to inward i_{NaCa}. Using this approach, Egan, Noble, Noble, Powell, Spindler & Twist (1989) predicted that inward i_{NaCa} flows during the plateau of the guinea-pig ventricular action potential thus delaying repolarization to 'some degree.' The technique cannot, however, measure i_{NaCa} *directly* at plateau potentials. More recently, LeGuennec & Noble (1994) approached the problem in another way: they partly blocked inward i_{NaCa} by rapidly replacing 50% of extracellular Na^+ with Li^+ during the action potential of guinea-pig ventricular cells. This resulted in a ~20% shortening of the action potential that may have resulted from the partial block of inward i_{NaCa}. However, changing extracellular Na^+

* To whom correspondence should be addressed.

is expected to alter intracellular Ca^{2+} and thus a variety of Ca^{2+}-dependent currents (i_{NaCa}; i_{Ca}; Ca^{2+}-activated Cl^- current, $i_{Cl(Ca)}$; delayed rectifier K^+ current, i_K; Ca^{2+}-activated non-specific cation current, $i_{Na,K(Ca)}$) and changes in these currents may have contributed to the shortening of the action potential.

In the present study we have measured i_{NaCa} at plateau potentials in ferret ventricular cells by blocking inward i_{NaCa} by replacing extracellular Na^+ with Li^+ or by substantially reducing the Ca^{2+} transient (by buffering intracellular Ca^{2+}). The contribution of inward i_{NaCa} to the action potential plateau has also been assessed. Contraction has been used as a measure of the intracellular Ca^{2+} transient so that changes in other Ca^{2+}-dependent currents can be taken into account. Conventional microelectrodes and the switch clamp technique were used to minimize intracellular dialysis and allow measurements to be made under physiological conditions.

Preliminary accounts of this work have been presented to The Physiological Society (Janvier, Boyett & Harrison, 1994; Janvier & Boyett, 1996*b*) and the Biophysical Society (Janvier & Boyett, 1996*c*).

METHODS

Experiments were performed on isolated ferret ventricular cells. A ferret was anaesthetized by intraperitoneal injection of 90–150 mg sodium pentobarbitone. The heart was rapidly excised and placed in 'isolation solution' (see below) containing 750 μM $CaCl_2$. The aorta was cannulated and the heart retrogradely perfused at ~20–23 ml min^{-1} with isolation solution containing 750 μM Ca^{2+} for sufficient time to clear all the blood (~2–3 min). The perfusate was then switched to Ca^{2+}-free isolation solution (containing 0·1 mM EGTA) for 4 min. Finally, the hearts were perfused for 10 min with 'enzyme solution': isolation solution containing 1 mg ml^{-1} collagenase (Worthington Type II, Lorne Laboratories), 0·1 mg ml^{-1} protease (Sigma) and 50 μM $CaCl_2$; this solution was recirculated through the heart. The ventricles were cut away from the atria, finely chopped, placed in a conical flask and digested with the enzyme solution supplemented with 10% (w/v) bovine serum albumin for a further 5 min. The tissue was shaken gently during this period. This process was repeated four times and the cells from each 5 min period were harvested by filtration and pelleted by centrifugation at 400 r.p.m. for 40 s. Cells were washed by resuspending them in isolation solution containing 750 μM Ca^{2+} and then recentrifuging them. The cells were stored in isolation solution containing 750 μM Ca^{2+} at 4 °C until required. The isolation procedure was performed at 37 °C. Isolation solution contained (mM): NaCl, 130; KCl, 5·4; $MgCl_2$, 1·4; NaH_2PO_4, 0·4; creatine, 10; taurine, 20; Hepes, 10; glucose, 10; pH 7. 3 at room temperature. This solution was equilibrated with O_2.

Cells were pipetted into a small tissue bath (volume, 0·2 ml) attached to the stage of an inverted microscope (Nikon Diaphot). The cells were allowed to settle for several minutes onto the glass bottom of the chamber before being superfused at a rate of ~1·6 ml min^{-1} with Tyrode solution of the following composition (mM): NaCl, 136·9; KCl, 5·4; $CaCl_2$, 2; $MgCl_2$, 0·57; NaH_2PO_4, 0·37; Hepes, 5; glucose, 5·6; pH 7·4 at 37 °C. In some experiments NaCl was replaced with LiCl at the same concentration to block inward i_{NaCa}. In this case the flow rate was increased to ~3 ml min^{-1} to reduce the solution exchange time in the chamber.

In other experiments 5 μM acetoxymethyl ester form of BAPTA (BAPTA AM) or 10^{-8} M isoprenaline was added to the Tyrode solution to buffer intracellular Ca^{2+} or increase the intracellular Ca^{2+} transient, respectively. A 1 mM BAPTA AM stock solution was made by dissolving the drug in dimethyl sulphoxide (DMSO). Cells were perfused with Tyrode solution containing 5 μM BAPTA AM (0·5% DMSO) for 5–10 min. During this period the size of the contraction dwindled as a result of the buffering of intracellular Ca^{2+}. When the contraction was almost completely abolished, the BAPTA AM was washed-off. On wash-off of BAPTA AM the contraction did not recover (BAPTA remained trapped within the cells as a result of the cleavage of the AM group by intracellular esterases). (As a control, cells were exposed to Tyrode solution containing 0·5% DMSO only for 10 min; this had no effect – $n = 4$.) Measurements were only made after more than 2 min of wash-off of BAPTA AM. A 10^{-6} M stock solution of isoprenaline was prepared. Both the stock solution and the Tyrode solution to which isoprenaline was added contained 40 μM EDTA to prevent oxidation of the drug. We also used 20 μM nifedipine, 100 μM DIDS and 3 mM 4-AP to block i_{Ca}, $i_{Cl(Ca)}$ and i_{to} (transient outward K^+ current), respectively. Nifedipine was dissolved in methanol to give a stock solution of 20 mM (the final concentration of methanol in Tyrode solution was 0·1%). 4-AP was dissolved in double-distilled water to give a final stock concentration of 300 mM. DIDS was added directly to Tyrode solution. In experiments involving DIDS, a cell was exposed to DIDS before and after application of BAPTA AM (e.g. Fig. 6). In early experiments involving DIDS, DIDS was also included in the BAPTA AM-containing Tyrode solution and, therefore, the cell was exposed to DIDS for up to 14 min. In later experiments, to minimize exposure time to DIDS, DIDS was omitted from the BAPTA AM-containing Tyrode solution and the cell was only exposed to DIDS for a total of 4 min. In both cases we obtained quantitatively similar results. The pH of Tyrode solution containing a drug was checked and re-adjusted if necessary.

Miniature solenoid valves (Lee Products Ltd, Gerrards Cross, Bucks, UK) controlled which of four solutions flowed to the chamber. The fluid level in the chamber was controlled using the system described by Cannell & Lederer (1986). The temperature of the solution was maintained at 37 ± 0·5°C by a heating coil wrapped around the glass inflow tube immediately prior to the chamber. Solution temperature was monitored by a thermistor mounted in the side of the chamber and controlled by a feedback circuit, which regulated the flow of current to the heating coil.

Ventricular cells were impaled with conventional microelectrodes (15–30 MΩ) filled with 1 M KCl. The switch clamp technique was used to voltage clamp cells (Dagan 8800 amplifier; switching frequency, ~4·5 kHz) to minimize intracellular dialysis and allow stable recordings of up to and over 1 h. The capacitance of the microelectrode was compensated just prior to impalement. The electrode potential upon switching between current injection and voltage recording was continuously monitored on an oscilloscope throughout an experiment to ensure that the electrode potential was stable during the measurement of membrane voltage. Membrane current was typically filtered at 1 kHz (low-pass filter). Membrane voltage and current were also displayed on an oscilloscope (Tektronix 5000 series) to assess the quality of the voltage clamp. Timing units (Hi-Med, Reading, UK) were used to control voltage clamp protocols and synchronize other recording equipment. A pulse generator (Boyett, Deane, Newcombe & Orchard, 1989) was used to drive the action potential clamp experiments. Briefly, action potentials at a stimulation rate of 1 Hz were recorded from a cell and an average of five were transferred to the pulse generator as a text file. The pulse generator was then used to apply the action

potential clamp waveform (via the Dagan 8800 amplifier) repetitively at a rate of 1 Hz. In experiments using a standard action potential waveform (see Fig. 10), the 'resting potential' during action potential clamp was changed to match the resting potential of the cell under control conditions.

Cell length was recorded using an optical system based on a photodiode array (Boyett, Moore, Jewell, Montgomery, Kirby & Orchard, 1988), and action potential duration was measured electronically at −65 mV (Kentish & Boyett, 1983). Membrane current and voltage, cell length, twitch shortening and action potential duration were displayed on a six-channel chart recorder (Gould 2600 S or RS 3600) and simultaneously recorded on video tape using a pulse code modulator (Neuro-Corder DR-890, Neuro Data Instruments Corp., New York) and a video recorder. Membrane current and voltage and cell length were also digitized using an analog to digital converter (1401 plus, Cambridge Electronic Design, Cambridge, UK) and stored on an IBM-compatible computer running the Cambridge Electronic Design voltage clamp software.

Cells were stimulated to contract by either a 5 ms current pulse (current clamp mode), a 150 or 200 ms voltage clamp pulse or application of the action potential clamp, at a range of frequencies.

Data are presented as means ± S.E.M.; n, number of cells.

RESULTS

Two methods were used to block inward i_{NaCa}: the replacement of Na^+ with Li^+ and buffering of intracellular Ca^{2+} by BAPTA AM. In each case we measured the effects on both the action potential and membrane current.

Experiments with Li^+-containing Tyrode solution

Figure 1 shows the effect of replacing extracellular Na^+ with Li^+ on the action potential and accompanying contraction. In these experiments Na^+-containing Tyrode solution was replaced by Li^+-containing solution between beats. To assess the time course of the solution switch we first replaced normal Tyrode solution with Tyrode solution containing 10 mM K^+, which caused a marked depolarization of the resting membrane potential and provided a useful measure of the time course of the switch. In eight cells the half-time of the solution switch was 1·4 ± 0·2 s. Each cell was stimulated at a sufficiently low rate to ensure complete exchange (as judged by the K^+-induced membrane depolarization) before the next beat. Exposure to Li^+ also caused a depolarization of the resting membrane potential (of ~2 mV in Fig. 1), which was used as a further check that the solution switch was complete between beats. In Fig. 1 the consecutive action potentials and contractions labelled 1 to 3 were recorded before (1), during (2) and after (3) a 6 s exposure to Li^+-containing solution. In this case the cell was stimulated once every 6 s (0·17 Hz). Li^+-containing solution was applied after beat 1 and washed off after beat 2.

Figure 1 shows that the action potential in the presence of Li^+ (2) was shorter than the preceding control (1). Mean results describing the effects of Li^+ substitution on action potential duration and contraction are shown in Fig. 2*A* – in nineteen cells the average action potential shortening was 56 ± 3 and 44 ± 2% at 0 and −65 mV, respectively, with stimulation rates of 0·25–0·1 Hz. Figure 1 also shows that the contraction in the presence of Li^+ (2) was potentiated as compared with the preceding control (1) (this is also confirmed by the mean results from fifteen cells in Fig. 2*A*). It could, therefore, be argued that the shortening of the action potential in the presence of Li^+-containing solution

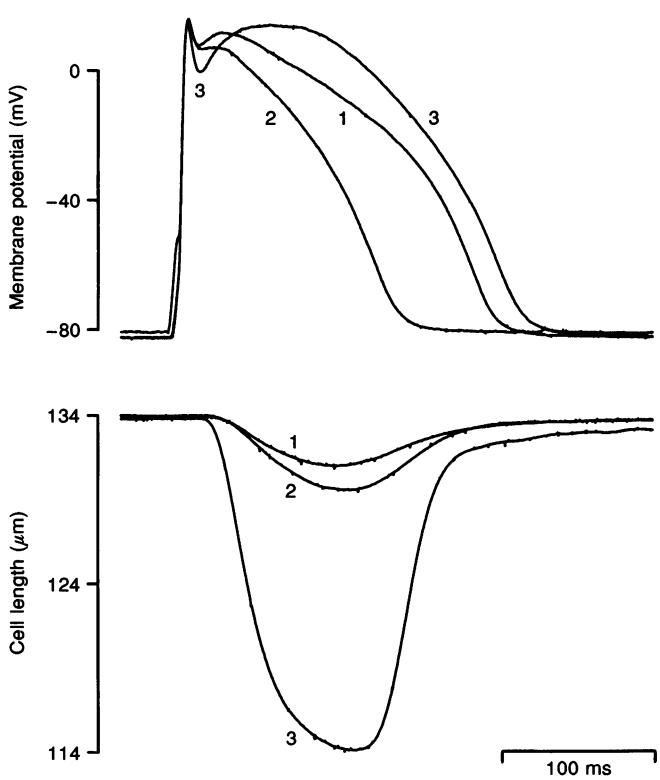

Figure 1. Effect of replacement of Na^+ with Li^+ on the action potential (top) and accompanying contraction (bottom)

The three responses (1–3) are consecutive beats at a rate of 0·17 Hz. The action potential and contraction labelled 1 were recorded under control conditions, 2 during and 3 after the wash-off of Li^+-containing Tyrode solution.

was not the result of the block of inward i_{NaCa} and instead was the result of a change in another Ca^{2+}-dependent current, such as a decrease in i_{Ca}, caused by a rise in intracellular Ca^{2+}. The contraction after the wash-off of Li^+, labelled 3, was strongly potentiated (Figs 1 and 2*A*). The underlying further increase in intracellular Ca^{2+} might be expected to result in a further decrease in i_{Ca} and shortening of the action potential. However the accompanying action potential (3) was *prolonged* compared with the control (1) (the action potential also displayed a prominent 'notch' at the start and a large 'dome') (Fig. 1). Action potential 3 was prolonged, on average, by 20 ± 6 and $9 \pm 2\%$ at 0 and -65 mV, respectively ($n = 19$), as shown in Fig. 2*A*. The prolongation of action potential 3 can be explained by an increase in inward i_{NaCa} as a result of the expected increase in the underlying intracellular Ca^{2+} transient. Consistent with this explanation, Fig. 2*A* shows that the contraction and duration of the action potential declined to control with a similar time course over beats 3 to 5.

In order to explain the changes in action potential shape and duration during and after Li^+ substitution, the effect of Li^+ on membrane current was investigated in voltage clamp experiments; a typical result is shown in Fig. 3. Membrane currents and contractions were recorded during 150 ms voltage clamp pulses from -80 to 0 mV, a potential that occurs approximately in the middle of the ferret ventricular action potential plateau. In the example shown in Fig. 3, the rate of stimulation was 0·2 Hz. Li^+-containing solution was again applied after beat 1 and washed-off after beat 2. The membrane current in the presence of Li^+, labelled 2, was more outward than the control, labelled 1. Current 2 has been subtracted from current 1 to obtain the Li^+-sensitive current which is displayed at the top of Fig. 3*B*, labelled 1 − 2. The difference current was inward throughout the voltage clamp pulse; it rapidly rose to a peak and then slowly decayed. In nine cells the difference current, 35 ms after the start of the pulse, had a magnitude of $0{\cdot}18 \pm 0{\cdot}03$ nA (measured with respect to zero) at 0·2 Hz.

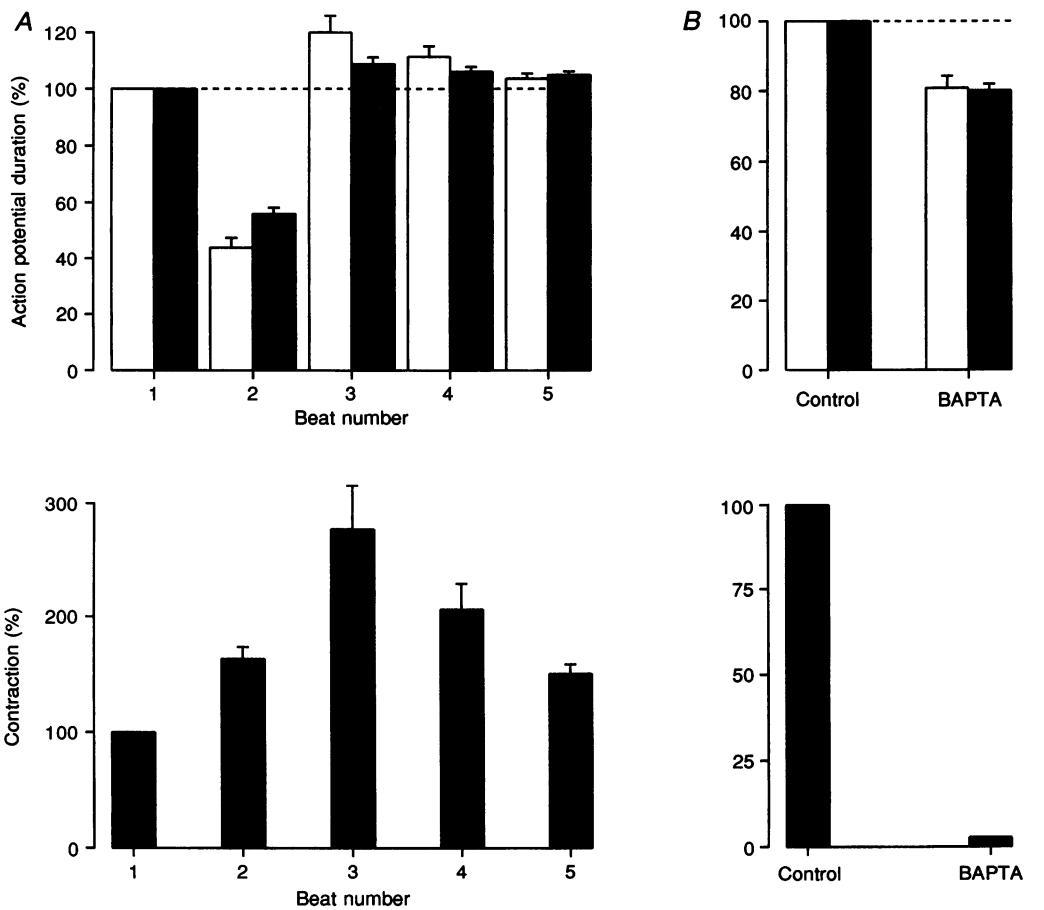

Figure 2. Summary of the effect of replacement of Na^+ with Li^+ and the buffering of intracellular Ca^{2+} by BAPTA AM on the action potential and contraction

A, effect of the replacement of Na^+ with Li^+ on action potential duration (top) and contraction (bottom). Data during beat 1 before, beat 2 during and beats 3, 4, and 5 after the wash-off of Li^+-containing Tyrode solution are shown. *B*, effect of buffering intracellular Ca^{2+} with BAPTA AM on action potential duration (top) and contraction (bottom). In the upper panels the open bars represent action potential duration at 0 mV and the closed bars represent action potential duration at -65 mV. All responses are expressed as a percentage of the response under control conditions. Means and S.E.M. shown ($n = 19$, 15, 37 and 32 for *A* top, *A* bottom, *B* top and *B* bottom, respectively).

Block of this inward component of membrane current in the presence of Li^+ can explain the shortening of the action potential seen in Fig. 1.

After the wash-off of Li^+, the contraction, labelled 3 in Fig. 3*A*, was potentiated and the accompanying membrane current, also labelled 3, was shifted inwards compared with the control (1). This extra inward current can also be seen in the two lower difference currents in Fig. 3*B* in which currents 1 or 2 have been subtracted from current 3. The difference current labelled 3 − 1 represents changes in membrane current at 0 mV which could be due *only* to the increase in the size of the Ca^{2+} transient, because Li^+ was absent during both beats. (However, a change in, for example, intracellular pH (Vaughan-Jones, Lederer & Eisner, 1983) during beat 3, as a result of the Li^+ exposure, theoretically, could also be involved.) In the case of the difference current 3 − 1, we routinely observed an early outward spike of current followed by a transient inward current which declined during the voltage clamp pulse. The outward spike of current could explain the more prominent notch at the start of action potential 3 in Fig. 1 and the inward current could explain its prolongation. The outward current may be $i_{Cl(Ca)}$ as explained below. The inward current may be inward i_{NaCa}. The form of the difference currents 1 − 2, 3 − 2 and 3 − 1 varied in a characteristic fashion as shown in Fig. 3*B*. The changes can be explained by the overlap of $i_{Cl(Ca)}$ and inward i_{NaCa} as explained in the Discussion.

Experiments with BAPTA AM

Next we investigated the effects of buffering intracellular Ca^{2+} with BAPTA AM on the action potential, membrane current and contraction at a rate of 1 Hz. After application and wash-off of 5 μM BAPTA AM (see Methods for details), the contraction was dramatically reduced compared with the control (Fig. 4*A*). BAPTA AM reduced contraction by $97 \pm 0{\cdot}2\%$ ($n = 32$). This reduction in contraction was accompanied by a significant shortening of the action potential (Fig. 4*A*); action potential duration was reduced by 19 ± 3 and $20 \pm 2\%$ at 0 and −65 mV, respectively ($n = 37$). Mean results for action potential duration and contraction are illustrated in Fig. 2*B*.

Figure 4*B* shows results from a typical voltage clamp experiment. Membrane current was recorded during 200 ms voltage clamp pulses from −80 to 0 mV at a rate of 1 Hz. Buffering intracellular Ca^{2+} caused an outward shift of current during the voltage-clamp pulse. The BAPTA-sensitive current (Control − BAPTA) is shown at the bottom

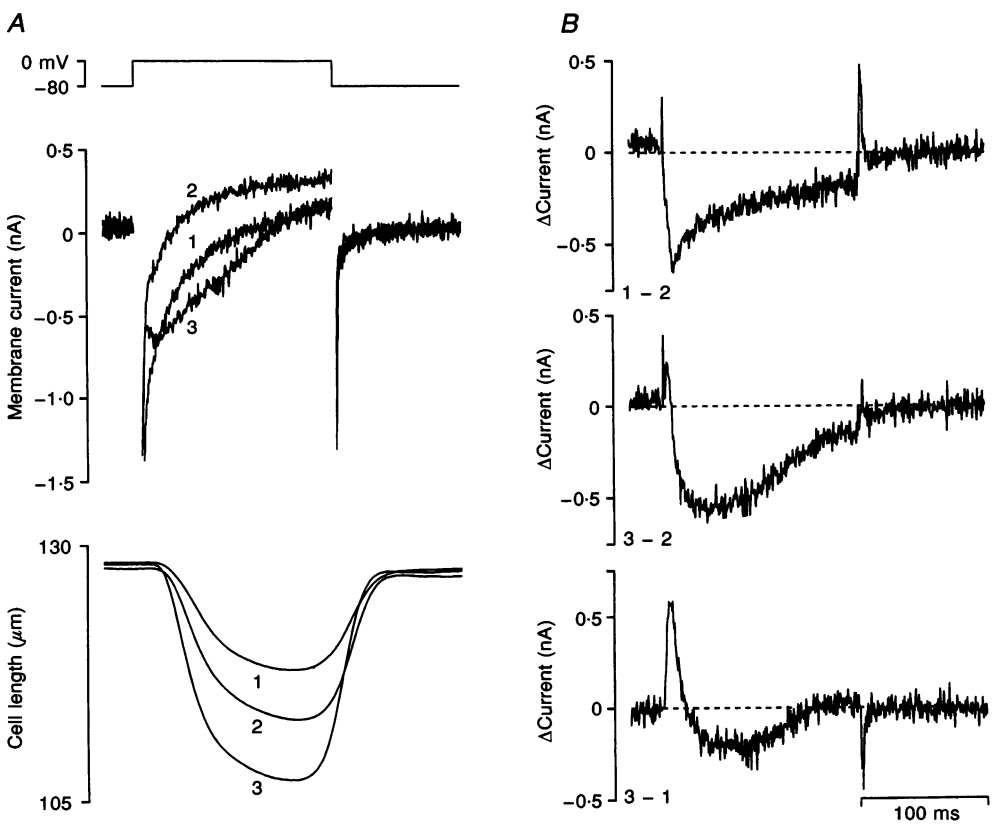

Figure 3. Effect of replacement of Na^+ with Li^+ on membrane current and contraction

A, membrane currents (middle) recorded during 150 ms voltage clamp pulses from −80 to 0 mV (top schematic) and the accompanying contractions (bottom). The three responses (1–3) are consecutive beats at a rate of 0·2 Hz. The responses labelled 1 were recorded under control conditions, 2 during and 3 after wash-off of Li^+-containing Tyrode solution. *B*, difference currents calculated by subtracting current 2 from 1 (top), 2 from 3 (middle) and 1 from 3 (bottom).

of Fig. 4*B*. As with the difference current 3 − 1 in Fig. 3*B*, we routinely observed a brief spike of outward current followed by a transient inward current. In thirty-one cells the peak inward current was 0·23 ± 0·02 nA (measured with respect to zero). The peak inward current occurred 30·9 ± 1·3 ms ($n = 31$) after the start of the pulse. The loss of this current is presumably responsible for the shortening of the action potential after the application of BAPTA AM.

Experiments with isoprenaline

To investigate further whether the inward BAPTA-sensitive current was Ca^{2+} dependent (i.e. as expected of inward i_{NaCa}) we increased contraction (and hence the Ca^{2+} transient) by the application of 10^{-8} M isoprenaline, before buffering intracellular Ca^{2+} with BAPTA AM. A typical result is shown in Fig. 5. Membrane current and contractions were recorded during 200 ms voltage clamp pulses from −80 to 0 mV at a rate of 1 Hz. The BAPTA-sensitive currents were recorded as before and are shown in the middle panel. Contractions under control conditions and after application of isoprenaline are shown in the bottom panel. In this experiment, contraction was increased by ~70% and the peak inward BAPTA-sensitive current was increased by ~65% after the application of isoprenaline. After the application of isoprenaline there was a pronounced double contraction during the voltage clamp pulse and the BAPTA-sensitive current *also* showed two inward peaks. In the presence of isoprenaline, in addition to the increase in inward current, the outward spike of current at the start of the voltage clamp pulse became broader compared with control. The results support the hypothesis that both currents (the outward spike of current and the transient inward current) are activated by intracellular Ca^{2+}. Further experiments to investigate the nature of these two currents were carried out.

Experiments with DIDS

A Ca^{2+}-activated Cl^- current ($i_{Cl(Ca)}$) is known to exist in cardiac muscle (Zygmunt & Gibbons, 1991). $i_{Cl(Ca)}$ is expected to be outward at 0 mV. To test if the outward spike of BAPTA-sensitive current (Figs 4 and 5) is $i_{Cl(Ca)}$ we investigated the effect of DIDS, a known Cl^- current blocker, on the current. Membrane current was recorded

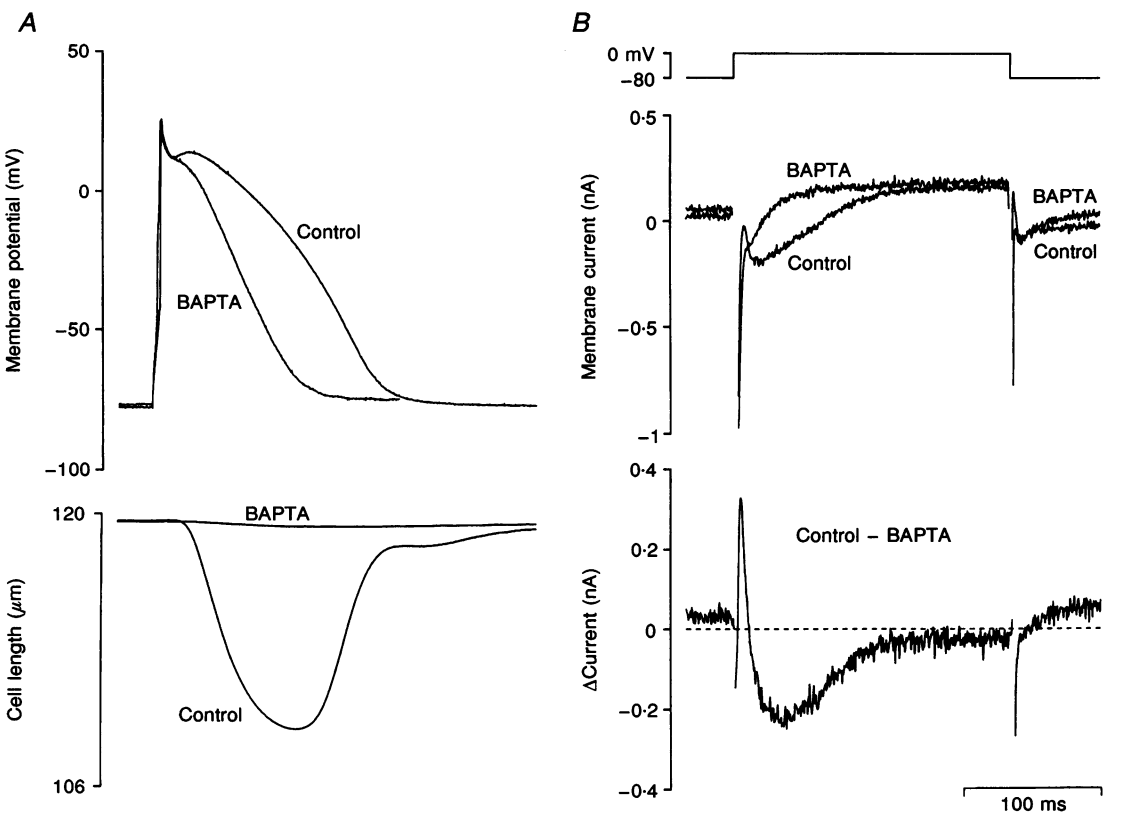

Figure 4. Effect of buffering intracellular Ca^{2+} by BAPTA AM on the action potential, the accompanying contraction and membrane current

A, superimposed action potentials (top) and contractions (bottom) under control conditions and after the application and wash-off of BAPTA AM. Traces are an average of five responses. *B*, membrane currents (middle) during a 200 ms voltage clamp pulse (top schematic) under control conditions and after the application and wash-off of BAPTA AM. The difference current in the lower part of *B* was calculated by subtracting the current after the application and wash-off of BAPTA AM from the current under control conditions. The traces are an average of ten responses. In this experiment and all subsequent ones using BAPTA AM, the stimulation rate was 1 Hz. The results shown in *A* and *B* were obtained from different cells.

during 200 ms pulses from −80 to 0 mV at a rate of 1 Hz. Figure 6*A* shows the effect of 100 μM DIDS on the BAPTA-sensitive current. The top of Fig. 6*A* shows a normal BAPTA-sensitive current, which was recorded in the same way as that in Fig. 4*B*, with the usual outward spike and transient inward currents. The middle trace in Fig. 6*A* shows the DIDS-sensitive current (from the same cell) which was obtained by subtracting membrane current in the presence of DIDS from the control current (before the application of BAPTA AM). The DIDS-sensitive current presumably represents $i_{Cl(Ca)}$ only and is similar in amplitude and time course to the outward spike of current in the top panel of Fig. 6*A*. The BAPTA-sensitive current in the presence of DIDS is shown at the bottom of Fig. 6*A*. This difference current was obtained by subtracting membrane current in the presence of DIDS and after the application of BAPTA AM from current in the presence of DIDS only. The difference current displays the usual transient inward current but no longer the outward spike. Similar results were seen in a total of seven cells.

$i_{Cl(Ca)}$ is believed to contribute to the early rapid phase of repolarization (phase 1) immediately after the upstroke of the action potential (Zygmunt & Gibbons, 1991). Its activation by the Ca^{2+} transient might therefore contribute to phase 1 repolarization and the notch at the start of the ferret ventricular action potential (e.g. Fig. 1). This notch is particularly prominent in action potential 3 in the type of experiment illustrated in Fig. 1. In this case the prominent notch can be explained by the large contraction (and therefore large Ca^{2+} transient) at this time: the expected increase in the Ca^{2+} transient is expected to activate more $i_{Cl(Ca)}$ causing an enhanced early rapid repolarization. Another experiment of this type is shown in the top panel of Fig. 6*B*. The cell was stimulated at 0·2 Hz. After the action potential labelled 1 was recorded, the cell was exposed to Li^+-containing solution for ~5 s as before. This was washed off prior to beat 3. As before, the contraction in beat 3 was augmented (not shown) and the accompanying action potential had a larger notch (Fig. 6*B*, top). After this result was obtained, the cell was exposed to 100 μM DIDS for 2 min and then Li^+-containing solution was briefly re-applied in the presence of DIDS. The result obtained is shown in the bottom panel of Fig. 6*B*. DIDS abolished both the small notch during action potential 1 and the augmented notch during action potential 3. Similar results were obtained from a total of four cells. These results show that $i_{Cl(Ca)}$ makes a contribution to phase 1 repolarization and the notch in ferret ventricular cells.

Current–voltage relationships for the BAPTA-sensitive and Li^+-sensitive inward currents

If the *inward* BAPTA-sensitive current is inward i_{NaCa} it should show the appropriate voltage dependence. A typical experiment to investigate the voltage dependence of the BAPTA-sensitive current is shown in Fig. 7*A*. The

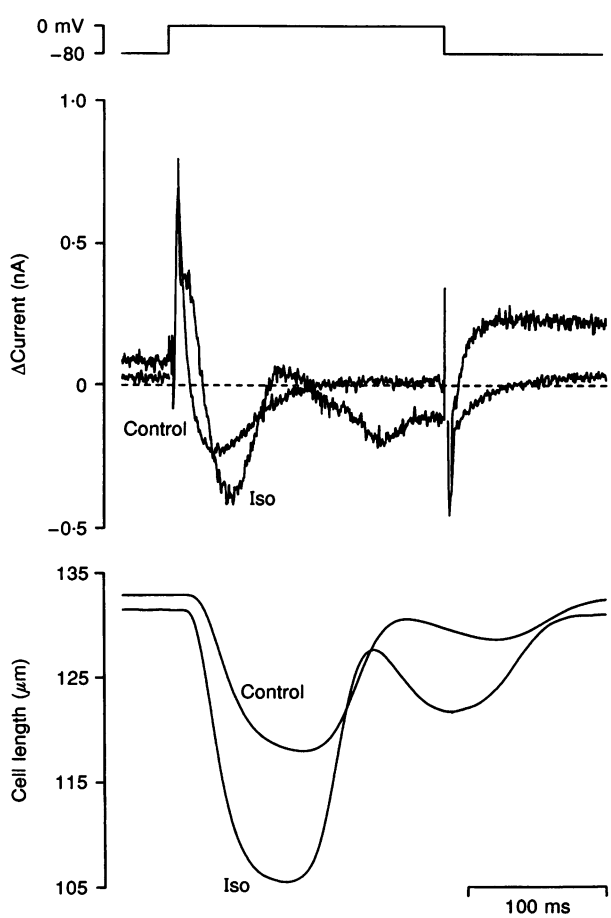

Figure 5. Effect of 10^{-8} M isoprenaline on the BAPTA-sensitive current and contraction

Superimposed BAPTA-sensitive currents (middle) and contractions (bottom) during a 200 ms voltage clamp pulse (top schematic) under control conditions and after the application of 10^{-8} M isoprenaline (Iso) are shown. The traces are an average of ten responses.

membrane potential was stepped from −80 to 0 mV and then 35 ms later, at approximately the peak of the inward current, it was stepped to one of four different test potentials: −80, −40, 0 or +40 mV. This was repeated before and after the application of BAPTA AM and the BAPTA-sensitive current was calculated by subtraction as described above. BAPTA-sensitive currents from one cell at the four test potentials are shown in Fig. 7*A*. A step to −80 or −40 mV produced a large inward tail current that decayed rapidly; at more positive potentials the tail current was smaller. The mean amplitudes of the tail currents measured in four experiments are plotted against the test potential in Fig. 7*B*. The inward current declined at more positive potentials.

In five cells the current–voltage relationship of the Li^+-sensitive current was measured as described above. Li^+-containing solution was applied for just one beat as in the experiment shown in Fig. 3. Current records in the presence of Li^+ were subtracted from current records under control conditions to obtain the Li^+-sensitive current. Like the inward BAPTA-sensitive current, the Li^+-sensitive current declined at more positive potentials (not shown).

Action potential clamp experiments

In the last series of experiments we used the action potential clamp technique to investigate the magnitude of the BAPTA-sensitive current *during an action potential*. In addition we measured the magnitude of the Ca^{2+} current (i_{Ca}) during the action potential so that the contributions of the two currents to the plateau can be compared.

The action potential clamp technique involves recording an action potential and using it as a voltage clamp command waveform. Figure 8*A* shows an action potential that was recorded from a ferret ventricular cell being stimulated at a rate of 1 Hz under control conditions. When this waveform was repetitively applied at a rate of 1 Hz to the same cell under voltage clamp control, almost zero current was recorded under control conditions as expected (Fig. 8*B*). Next BAPTA AM was briefly applied to the cell to buffer intracellular Ca^{2+}. The action potential after the application of BAPTA AM (Fig. 8*A*) was shorter than the control as described previously (Fig. 4*A*); in addition, after the application of BAPTA AM the action potential had a smaller notch consistent with a reduction in $i_{Cl(Ca)}$. After the application of BAPTA AM when the *control action potential*

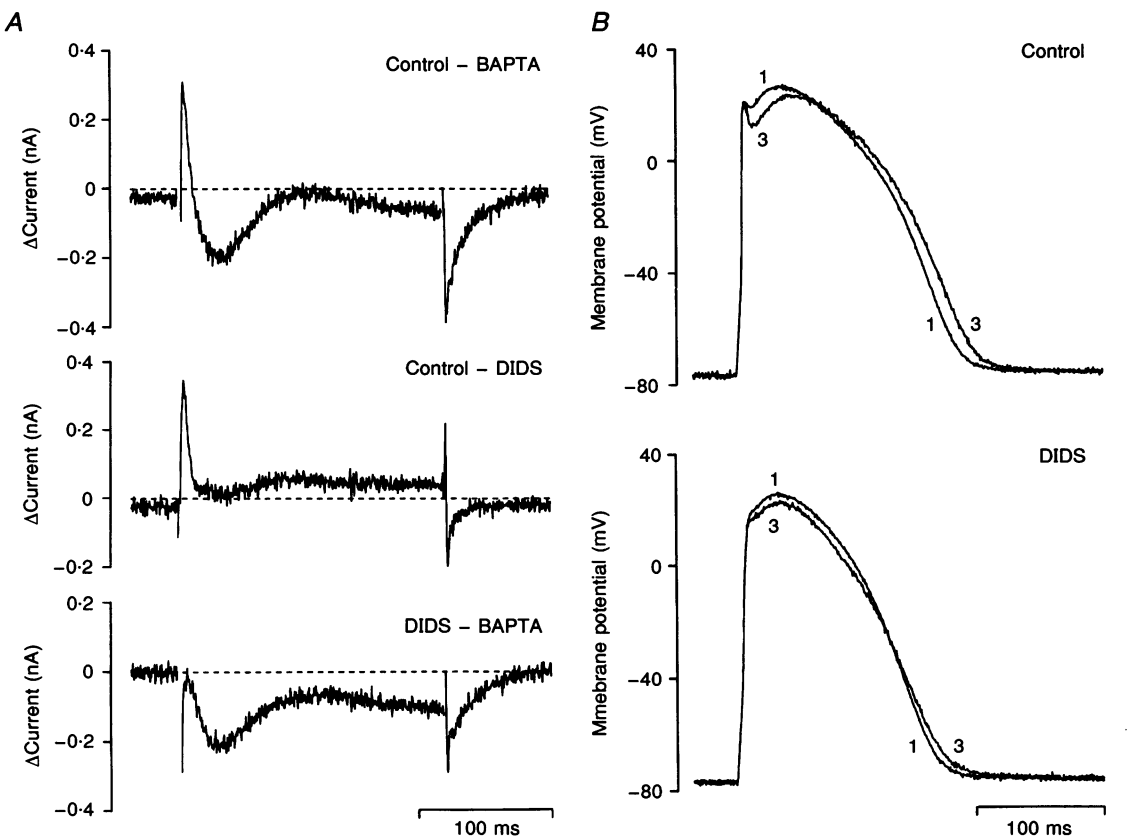

Figure 6. Effect of 100 μM DIDS on the BAPTA-sensitive current and action potential

A, BAPTA-sensitive current (top), DIDS-sensitive current (middle) and BAPTA-sensitive current in the presence of 100 μM DIDS (bottom). All currents were recorded during 200 ms voltage clamp pulses from −80 to 0 mV. See text for further explanation. The traces are an average of ten responses. *B*, action potentials before (1) and after (3) a 5 s exposure to Li^+-containing Tyrode solution under control conditions (top) and after a 2 min exposure to 100 μM DIDS (bottom). The action potentials shown are the first and third in a sequence at a rate of 0·2 Hz.

waveform (Fig. 8*A*) was applied to the cell under voltage clamp control, the current (Fig. 8*B*) was outwards for the majority of the action potential clamp waveform. This is analogous to the outward shift in current seen in the top panel of Fig. 4*B*. The BAPTA-sensitive current (Control – BAPTA) is shown in Fig. 8*C*. Like the BAPTA-sensitive current in earlier figures (e.g. Fig. 4), the current displays an outward spike followed by a transient inward current which flows for the majority of the action potential clamp waveform. Removal of the outward and inward currents in Fig. 8*C* by buffering intracellular Ca^{2+} can explain the observed effects on the action potential in Fig. 8*A*.

The current–voltage relationship of the *inward* BAPTA-sensitive current was obtained by plotting the magnitude of the current against membrane potential during the action potential clamp waveform. This is shown in Fig. 8*D*. The inward current was largest at positive potentials and declined at more negative potentials at later times during the action potential clamp waveform. This is markedly different from the current–voltage relationship in Fig. 7*B* and can be explained by the decline in the intracellular Ca^{2+} concentration during the action potential (see Discussion).

Figure 9 shows results from an experiment similar to that in Fig. 8. Action potentials under control conditions and after the application and wash-off of BAPTA AM are shown in Fig. 9*A* and the BAPTA-sensitive current during the control action potential waveform is shown in Fig. 9*B*; the current is similar to that in Fig. 8*C*, although there was little or no outward spike of current in this example. In this case, after the BAPTA AM was applied and washed off, the cell was exposed to 20 μM nifedipine to block i_{Ca}. The action potential in the presence of nifedipine (Fig. 9*A*) was shorter than the other action potentials and had a lower plateau. In the presence of nifedipine the control action potential waveform was applied to the cell under voltage clamp control. Figure 9*C* shows the nifedipine-sensitive current (presumably i_{Ca}) during the control action potential clamp waveform: the current recorded after the application and wash-off of BAPTA AM was subtracted from the current recorded after the further application of nifedipine. After the early inward peak of i_{Ca} the current (identified by the arrow) during the plateau of the action potential was similar in size to the inward BAPTA-sensitive current at the same time (cf. Fig. 9*B* and *C*).

At steady state, Ca^{2+} influx and efflux should be equal. It follows from this that the Ca^{2+} fluxes via the Ca^{2+} channel and the Na^+–Ca^{2+} exchanger during the action potential should be approximately equal if these two fluxes are more important than Ca^{2+} fluxes via other routes or during diastole. Figure 9*D* is a plot of Ca^{2+} influx via the Ca^{2+} channel and putative Ca^{2+} efflux via the Na^+–Ca^{2+} exchanger at a given time during the action potential clamp waveform. The fluxes were obtained by integrating the currents in Fig. 9*B* and *C*. In the case of the BAPTA-

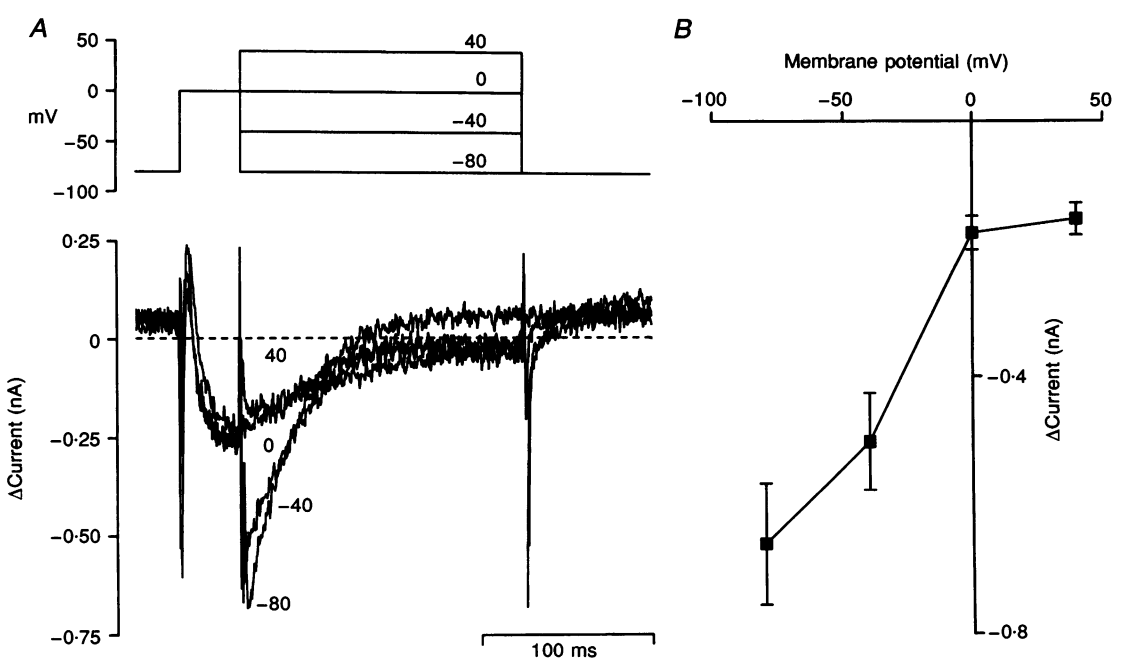

Figure 7. Current–voltage relationship of the inward BAPTA-sensitive current

A, voltage clamp protocol. Membrane potential (top schematic) and BAPTA-sensitive currents (bottom) are shown. Membrane potential was clamped to 0 mV for 35 ms and then to one of four different test potentials. The traces are an average of two responses. *B*, mean ± S.E.M. amplitude of the BAPTA-sensitive current measured in four cells from experiments like that in *A* plotted against membrane potential. The peak inward BAPTA-sensitive current was measured at each test potential. Current was measured with respect to zero.

sensitive current (putative inward i_{NaCa}; Fig. 9*B*), the dotted line was used as the baseline and the integral was multiplied by two to compensate for the single charge movement for each Ca^{2+} ejected. In the case of nifedipine-sensitive current (i_{Ca}), the current was measured with respect to zero. As predicted, the Ca^{2+} influx via i_{Ca}, labelled BAPTA − Nifedipine, was roughly equal to the putative Ca^{2+} efflux via the Na^+–Ca^{2+} exchanger, labelled (Control − BAPTA) × 2.

The effect of action potential shape on the BAPTA-sensitive current and i_{Ca}

Figure 9*C* shows that i_{Ca} reached a peak early during the ferret ventricular action potential and then subsequently declined. In contrast, Grantham & Cannell (1995) have reported that, in guinea-pig ventricular cells, i_{Ca} (measured with the action potential clamp technique) is small during the initial phase of the action potential and then reaches a peak later on as the cell repolarizes. It is possible that the difference in the profile of i_{Ca} is the result of differences in the action potential in the two species: the guinea-pig ventricular action potential displays a high plateau at ~+40 mV, whereas the plateau of the ferret ventricular action potential is relatively low (~+20 mV). The driving force for i_{Ca} and inward i_{NaCa} (*for a given* Ca^{2+} *transient*) is greater the lower, and therefore the more negative, the action potential plateau. It follows that altering the height of the plateau should alter the time course and magnitude of the two currents.

One important difference between the guinea-pig and ferret ventricular action potential is that the guinea-pig has little transient outward K^+ current (i_{to}). By blocking i_{to} with 4-AP it is possible to mimic the guinea-pig action potential in ferret cells. Figure 10 shows the results of experiments in which the BAPTA-sensitive current and i_{Ca} were recorded using the action potential clamp technique in the same way as before (once again nifedipine was applied only *after* intracellular Ca^{2+} had been buffered by application of BAPTA AM). The currents were recorded either during a

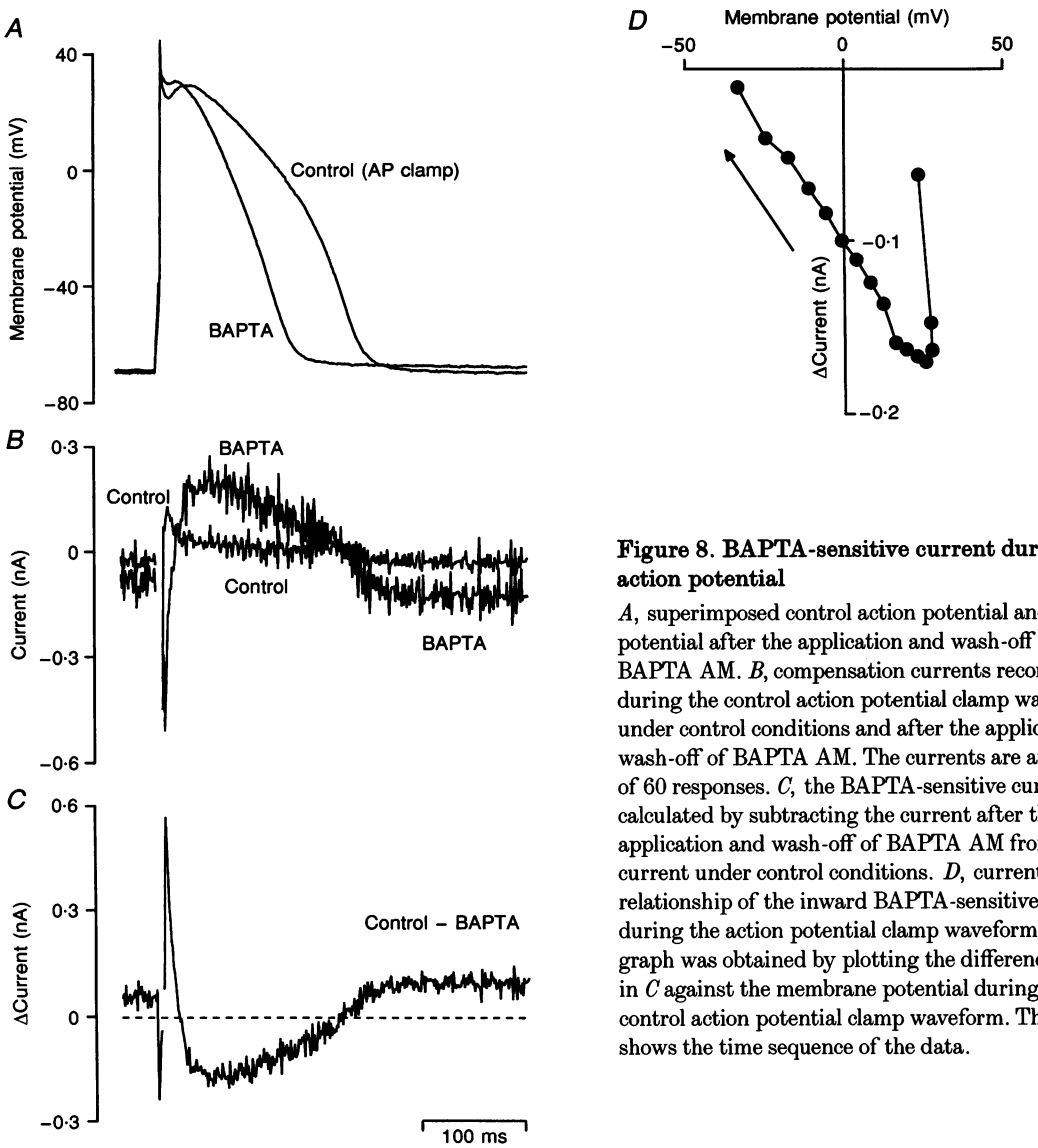

Figure 8. BAPTA-sensitive current during the action potential

A, superimposed control action potential and action potential after the application and wash-off of BAPTA AM. *B*, compensation currents recorded during the control action potential clamp waveform under control conditions and after the application and wash-off of BAPTA AM. The currents are an average of 60 responses. *C*, the BAPTA-sensitive current calculated by subtracting the current after the application and wash-off of BAPTA AM from the current under control conditions. *D*, current–voltage relationship of the inward BAPTA-sensitive current during the action potential clamp waveform. The graph was obtained by plotting the difference current in *C* against the membrane potential during the control action potential clamp waveform. The arrow shows the time sequence of the data.

control action potential clamp waveform (Fig. 10*A* and *B*, middle panels) or during an action potential recorded in the presence of 3 mM 4-AP (Fig. 10*A* and *B*, lower panels). By abolishing i_{to}, 4-AP increased the action potential overshoot from ~+25 to ~+45 mV and shifted the plateau to more positive potentials. During the control action potential clamp waveform the two currents were similar in profile to those in Fig. 9, whereas during the 4-AP waveform the profiles of the two currents were greatly altered: the inward BAPTA-sensitive current was significantly less than under normal conditions and displayed two peaks (these differences are considered in the Discussion) and i_{Ca} reached a peak late during the action potential. In six cells, in which intracellular Ca^{2+} was not buffered, the latency time of contraction (measured as the time between the upstroke of the action potential clamp and the start of contraction) was increased by 2·5 ± 0·6 ms (10·3 ± 2·3%) and the time to peak of contraction was slowed by 7·6 ± 1·5 ms (8·4 ± 1·8%) when the 4-AP action potential was used as the voltage-clamp command waveform instead of the control action potential.

DISCUSSION

Specificity of reagents

We have investigated the role of inward i_{NaCa} in the ferret ventricular action potential. Two methods were selected to reduce inward i_{NaCa}: the first was the replacement of extracellular Na^+ with Li^+. Li^+ cannot be carried by the exchanger and such a manoeuvre abolishes inward exchange current. Secondly, we buffered intracellular Ca^{2+} with BAPTA AM; this reduces the Ca^{2+} transient and therefore the component of inward i_{NaCa} triggered by the Ca^{2+} transient. Both of these methods have been used by others to abolish inward i_{NaCa} (e.g. Mitchell *et al.* 1984; LeGuennec & Noble, 1994; Lietch & Brown, 1996; for review see Janvier & Boyett, 1996*a*). For example, both methods have been used to demonstrate that the low plateau of the atrial or rat ventricular action potential is generated by inward i_{NaCa}. Nevertheless, before any conclusions can be drawn from the results, the specificity of Li^+ substitution and buffering Ca^{2+}, on the exchanger, must be considered. The TTX-sensitive Na^+ current has an almost equal permeability for Li^+ and Na^+ (Hille, 1992) and replacement of Na^+ by Li^+

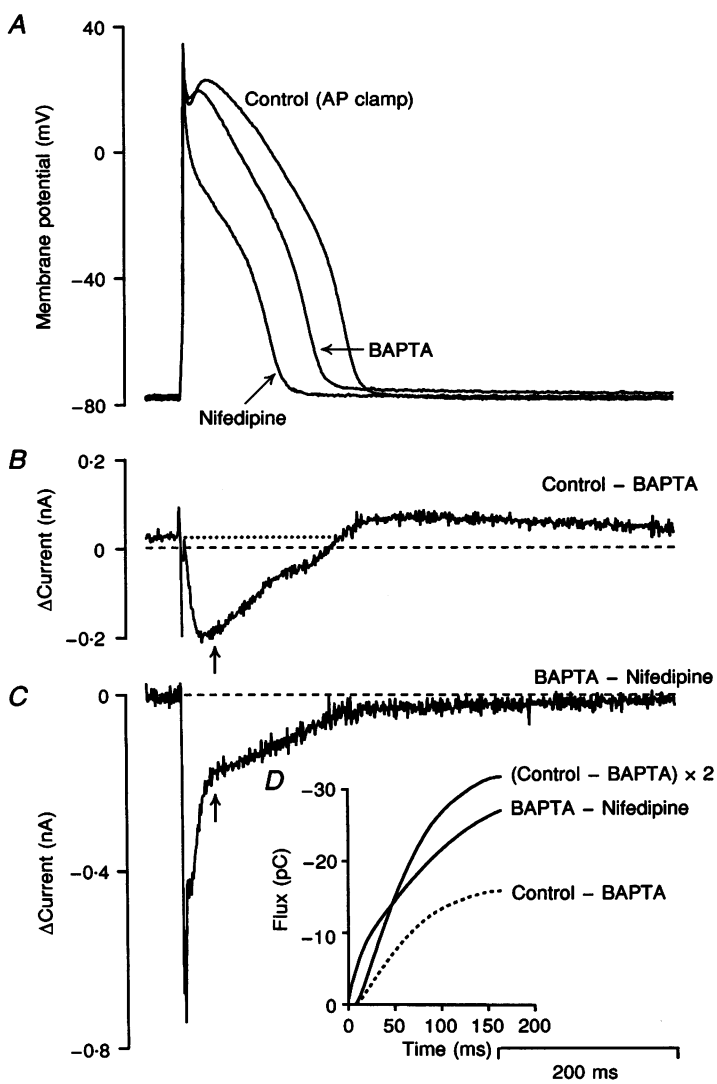

Figure 9. Comparison of the BAPTA- and nifedipine-sensitive currents during the action potential

A, control action potential and action potentials after the application and wash-off of BAPTA AM and then nifedipine. *B*, BAPTA-sensitive current, calculated by subtracting compensation current under control conditions from compensation current in the presence of BAPTA. Compensation currents were recorded during a control action potential clamp waveform (Control in *A*). *C*, nifedipine-sensitive current, calculated by subtracting compensation current in the presence of BAPTA alone from compensation current in the presence of BAPTA and nifedipine. *D*, Ca^{2+} flux (in pC) through Ca^{2+} channels and the Na^+–Ca^{2+} exchanger at different times during the control action potential clamp waveform. See text for further explanation.

does not significantly affect the background Na^+ current (Kiyosue, Spindler, Noble & Noble, 1993) or $i_{Na,K(Ca)}$ (Ehara, Noma & Ono, 1988). Any effects of Li^+-containing solution on the action potential cannot, therefore, be explained in terms of changes in these currents. Replacement of extracellular Na^+ by Li^+ is known to reduce the inward rectifier K^+ current, $i_{K,1}$ (Spindler, Noble & Noble, 1995). This can explain the depolarization of the resting membrane in the presence of Li^+ (Fig. 1), but it cannot explain the shortening of the action potential or the change in membrane current at 0 mV ($i_{K,1}$ is negligible at 0 mV) in the presence of Li^+. By blocking the Na^+–Ca^{2+} exchanger (the major Ca^{2+}-efflux pathway of the cell) Li^+-containing solution can elevate the intracellular Ca^{2+} concentration. Such an action explains the elevated contractions both in the presence and after the wash-off of Li^+-containing solution in this study (Figs 1–3). Any change in the magnitude of the Ca^{2+} transient may alter a variety of Ca^{2+}-dependent currents. Elevation of the Ca^{2+} transient may decrease peak i_{Ca} and increase its Ca^{2+}-dependent inactivation (Lee, Marban & Tsien, 1985) as well as activating $i_{Cl(Ca)}$ (Zygmunt & Gibbons, 1991), i_K (Tohse, 1990), $i_{Na,K(Ca)}$ (Ehara *et al.* 1988) and inward i_{NaCa} (Miura & Kimura, 1989). Buffering intracellular Ca^{2+} with BAPTA-AM, on the other hand, is expected to have the opposite effect on the currents. All of these effects must be taken into account when discussing the results.

Effect of Li^+ on membrane current

The direct effect of Li^+ substitution on membrane current is complicated by the accompanying changes in contraction (and therefore the underlying Ca^{2+} transient) during and after the substitution (as mentioned above). The Li^+-sensitive currents in Fig. 3*B* display an early spike of current in either an inward (1 – 2) or outward (3 – 2 and 3 – 1) direction. The early spike can be explained by $i_{Cl(Ca)}$, an outward current triggered by the Ca^{2+} transient. In the difference currents shown in Fig. 3*B*, the direction of the

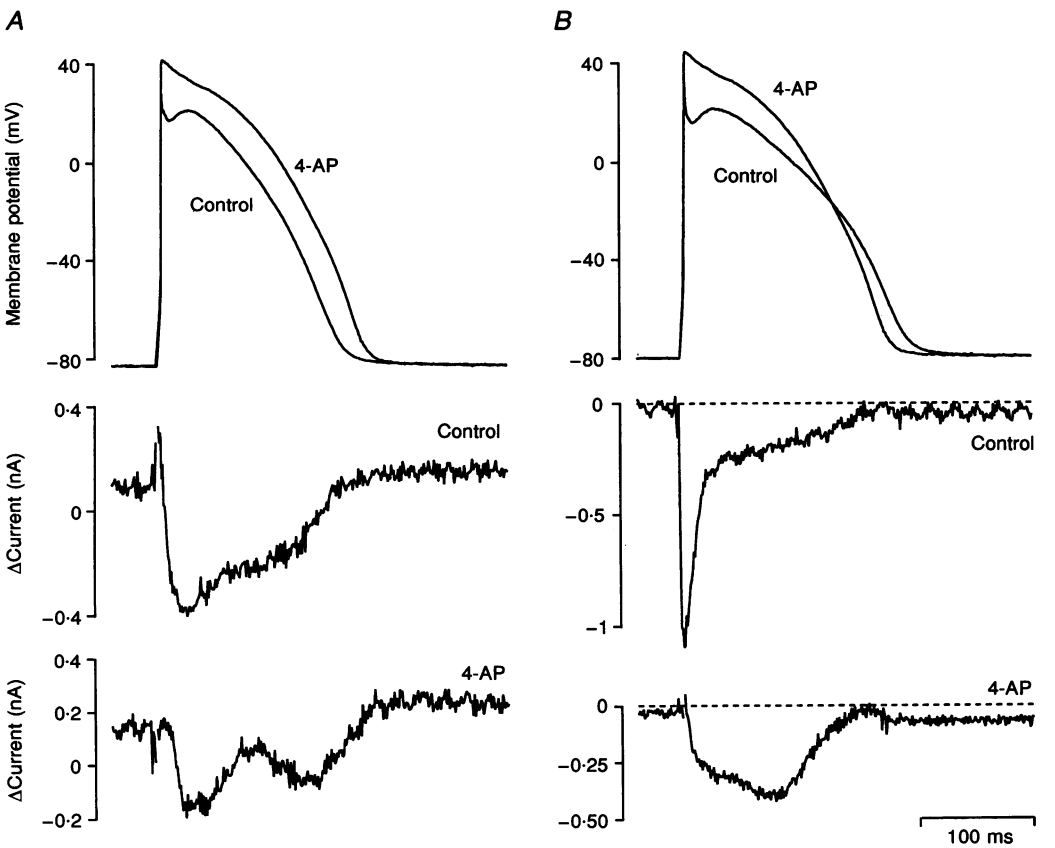

Figure 10. Effect of action potential shape on the BAPTA-sensitive current and i_{Ca}

A, BAPTA-sensitive current during action potentials of different shape. Top, superimposed action potential clamp waveforms under control conditions and in the presence of 3 mM 4-AP. The 4-AP action potential clamp waveform was recorded from a different cell. Middle, BAPTA-sensitive current recorded during the control action potential clamp waveform. Bottom, BAPTA-sensitive current recorded during the 4-AP action potential clamp waveform. *B*, i_{Ca} during action potentials of different shape. Top, superimposed action potential clamp waveforms under control conditions and in the presence of 3 mM 4-AP. The control and 4-AP action potential clamp waveforms were recorded from different cells; the 4-AP action potential clamp waveform is the same as that in *A*. Middle, nifedipine-sensitive current recorded during the control action potential clamp waveform. Bottom, nifedipine-sensitive current recorded during the 4-AP action potential clamp waveform.

early current depends on the relative size of the contraction (and thus Ca^{2+} transient) during each voltage clamp pulse used in the subtraction protocol: the top current in Fig. 3*B* is calculated as 1 − 2; in this case contraction 2 is bigger than 1 and the current is inward. The reverse is true for both 3 − 2 and 3 − 1. In the case of 3 − 2 and 3 − 1, the difference in contraction size is greatest for 3 − 1 and the early current is also greatest in this case. In every case in Fig. 3*B*, the difference currents display an inward component following the early spike. The inward current is transient in nature and may represent inward i_{NaCa} triggered by the Ca^{2+} transient (it had the current–voltage relationship expected of inward i_{NaCa}). The inward current cannot be explained by changes in i_{Ca}, i_K or $i_{Na,K(Ca)}$ as a result of changes in intracellular Ca^{2+}. For example, the changes in i_{Ca}, i_K and $i_{Na,K(Ca)}$ are expected to be greater in beat 3 than in beat 2, whereas the primary effect of Li^+ substitution on membrane current (the outward shift during beat 2) was reversed by beat 3. On the other hand, such changes are expected of inward i_{NaCa}: inward i_{NaCa} will be abolished during beat 2, but not beat 3. Furthermore, during beat 3, inward i_{NaCa} is expected to be greater than that in beat 1 (as a result of a larger Ca^{2+} transient) and evidence of this is seen in Fig. 3 (e.g. the difference current labelled 3 − 1).

Effect of buffering intracellular Ca^{2+} on membrane current

The BAPTA-sensitive current in Fig. 4*B* appears to be composed of two Ca^{2+}-activated currents. Both the early spike of outward current and the transient inward current were elevated when contraction, and therefore the underlying Ca^{2+} transient, was increased by the application of 10^{-8} M isoprenaline, as shown in Fig. 5. Furthermore, the early spike of BAPTA-sensitive current is similar in amplitude and time course to the early spike of Li^+-sensitive current; as discussed above, the early spike of Li^+-sensitive current is also likely to be Ca^{2+} activated. The early outward BAPTA-sensitive current was blocked by DIDS (Fig. 6), which suggests that it is a Cl^- current (the experiment in Fig. 6*A* also shows that it is independent of the subsequent inward current). The early outward current may be the DIDS-sensitive Ca^{2+}-activated Cl^- current, $i_{Cl(Ca)}$, first described by Zygmunt & Gibbons (1991). The BAPTA-sensitive inward current may represent i_{NaCa}: it rose to a peak in ~30 ms and then declined. The time course of the current is therefore similar to the underlying Ca^{2+} transient measured in other studies using fluorescent probes or Ca^{2+} tail currents (Terrar & White, 1989; Cheng, Cannell & Lederer, 1994). The current is also similar (in amplitude and time course) to the inward component of Li^+-sensitive current (Fig. 1). The BAPTA-sensitive inward current was voltage dependent and, like the Li^+-sensitive inward current, declined at more positive potentials (Fig. 7*B*) as expected of inward i_{NaCa}. Although, the almost complete elimination of the Ca^{2+} transient by buffering intracellular Ca^{2+} with BAPTA is also expected to enhance i_{Ca} and depress i_K and $i_{Na,K(Ca)}$, these changes are unlikely to be responsible for the BAPTA-sensitive inward current: although the depression of $i_{Na,K(Ca)}$ (if present in ferret ventricular cells) will generate a BAPTA-sensitive inward current, it is expected to reverse at ~0 mV and this was not the case (Figs 7*B* and 8*D*). The enhancement of i_{Ca} and depression of i_K cannot explain the BAPTA-sensitive inward current at 0 mV, because both changes would generate BAPTA-sensitive outward currents. However, a BAPTA-sensitive *outward* current was present at the holding potential in most experiments (Figs 4*B*, 5, 7*A*, 8*C*, 9*B* and 10*A*). This may be the result of a depression of i_K after the buffering of intracellular Ca^{2+} by BAPTA (Tohse, 1990). Three lines of evidence support this view: first, the current was greater after a voltage clamp pulse or action potential than before (i_K is activated by depolarization) (e.g. Figs 4*B* and 9*B*); secondly, the current was greater after an action potential with a higher plateau (Fig. 10*A*) and, finally, isoprenaline increased the magnitude of the current (Fig. 5). If this interpretation is correct, the BAPTA-induced inhibition of i_K at *0 mV* in experiments like that in Fig. 4*B* will partly offset the BAPTA-induced inhibition of i_{NaCa}; as a result i_{NaCa} will be underestimated. Because of these considerations the dotted line rather than the dashed line in Fig. 9*B* was used as the baseline for the integration of the inward BAPTA-sensitive current.

Effects of Li^+ and buffering intracellular Ca^{2+} on the action potential

The shortening of the action potential in the presence of Li^+ and the prolongation on wash-off (Fig. 1*A*) can be accounted for by the Li^+-dependent changes in membrane current at 0 mV (Fig. 1*B*). As discussed above, the Li^+-dependent changes in membrane current at 0 mV (apart from the early spike) are likely to be the result of changes in i_{NaCa}. The results suggest an important role for inward i_{NaCa} in controlling action potential duration. The prolonged action potential on wash-off of Li^+ also displayed a prominent notch at its start which was blocked by DIDS (Fig. 6*B*). This result suggests that the notch was generated by a prominent $i_{Cl(Ca)}$ activated by the larger Ca^{2+} transient presumably underlying the larger contraction.

Buffering intracellular Ca^{2+} with BAPTA AM shortened the action potential and often reduced the notch at its start (e.g. Figs 9 and 10). These effects can be explained by the BAPTA-dependent changes in membrane current (e.g. Figs 4*B* and 8*C*). As discussed above, the early spike of BAPTA-sensitive current is likely to be $i_{Cl(Ca)}$ and the loss of this current can explain the reduction of the notch sometimes observed after the application of BAPTA AM. The BAPTA-sensitive inward current is likely to be i_{NaCa} and the loss of this current can explain the shortening of the action potential. As well as the effects on the action potential mentioned above, buffering intracellular Ca^{2+} with BAPTA AM also routinely promoted a small depolarization of the resting membrane and slowed the very final phase of repolarization of the cell. Such effects can be seen in Figs 8

and 9 and may be explained by the possible reduction in i_K discussed above. If i_K is reduced by the buffering of Ca^{2+} then the resulting change in current will tend to *prolong* the action potential. In this case the shortening of the action potential in the presence of BAPTA of ~20% underestimates the role played by i_{NaCa} in the action potential.

Action potential clamp

Underlying the conclusion that i_{NaCa} helps to maintain the action potential plateau is the assumption that significant inward i_{NaCa} flows during the plateau phase. Using the action potential clamp technique we have confirmed that putative inward i_{NaCa} flows at both positive and negative potentials *throughout* the action potential plateau (Fig. 8). Perhaps surprisingly, Fig. 9 shows that for much of the plateau i_{NaCa} and i_{Ca} were roughly equal in size and thus their contributions to the plateau will be roughly equal. Figure 8*D* shows that during the action potential i_{NaCa} was maximal at positive potentials and declined at more negative potentials – this is opposite to the expected voltage dependence of the exchanger (shown in Fig. 7*B*). During the action potential the decline in i_{NaCa} at more negative potentials can be explained by the decline in the intracellular Ca^{2+} concentration, whereas in the experiment shown in Fig. 7 i_{NaCa} was presumably measured at a constant level of intracellular Ca^{2+} because, for each point, contraction (before application of BAPTA AM) was the same and always interrupted at the same time. It is concluded that during the ferret ventricular action potential, intracellular Ca^{2+} is a more important determinant of inward i_{NaCa} than membrane potential. The ventricular action potential of other species, notably the guinea-pig, have higher plateaus with less of a notch at the start. Figure 10 shows that in this type of action potential, inward i_{NaCa} (and i_{Ca}) will be smaller (although this does not necessarily mean that it will be less important).

Relation to other studies

A shortening of the action potential has been reported in other studies on removal of Na^+ (Mitchell *et al.* 1984; Horackova, Beresewicz & Isenberg, 1988; LeGuennec & Noble, 1994; for review see Janvier & Boyett, 1996*a*). A reduction in inward i_{NaCa} is expected to have contributed to the action potential shortening in these cases, but a Ca^{2+}-dependent change in another membrane current (especially a reduction in i_{Ca} – Boyett, Kirby & Orchard, 1988) may also have contributed if the Na^+ was removed for a prolonged period and thus the rise in intracellular Ca^{2+} was great. In the study of LeGuennec & Noble (1994) 50% of Na^+ was removed (replaced by Li^+) in ~50 ms at the start of a guinea-pig ventricular action potential. This is likely to have resulted in little or no rise in intracellular Ca^{2+} during the action potential and yet it resulted in a ~20% shortening of the action potential. In other studies, buffering intracellular Ca^{2+} has resulted in a shortening or a prolongation of the action potential (e.g. Mitchell *et al.* 1984; Terrar & White, 1989; for review see Janvier & Boyett, 1996*a*). These contradictory results can perhaps be explained by the degree of Ca^{2+} buffering. In the present study, a small contraction ($3 \pm 0{\cdot}2$% of control) remained after the application of 5 μM BAPTA AM and thus the intracellular Ca^{2+} concentration was likely to have been close to the threshold for contraction, i.e. ~10^{-7} M (it is possible that intracellular Ca^{2+} is $>10^{-7}$ M – see Kirshenlohr *et al.* 1994). In the present study, as well as in the study of Leitch & Brown (1996) on guinea-pig ventricular cells, 5 μM BAPTA AM resulted in a shortening of the action potential of ~20%. In studies in which a prolongation of the action potential was observed, the degree of Ca^{2+} buffering was greater. For example, LeGuennec & Noble (1994) observed a ~128% prolongation of the action potential at room temperature when intracellular Ca^{2+} was buffered by 30 mM BAPTA free acid in the patch pipette. At 35–36 °C Leitch & Brown (1996) measured a more modest, though still significant, prolongation of the action potential of 14% with 20 mM BAPTA free acid in the patch pipette. We estimate that the intracellular free Ca^{2+} concentration under these conditions is less than 10^{-9} M. Under these conditions Leitch & Brown (1996) showed that the inactivation of the Ca^{2+} current is prolonged (it was not significantly prolonged after the application of 5 μM BAPTA AM) and this can explain the prolongation of the action potential under these conditions. Egan *et al.* (1989) calculated that inward i_{NaCa} during the guinea-pig ventricular action potential was similar in amplitude (~0·2 nA) and time course to that in Fig. 8. The calculations were based on inward tail currents (presumed to be i_{NaCa}) measured when the action potential was interrupted at different times and clamped to the resting potential of the cell. In one respect, this is unexpected, because the present study suggests that the current would be more like that in the lower part of Fig. 10*A*. However, as Noble & Bett (1993) acknowledged, the calculation of inward i_{NaCa} is dependent on the assumed value of intracellular Na^+. In the Oxsoft model of the guinea-pig ventricular action potential, i_{NaCa} is biphasic like that in the lower part of Fig. 9*A* (see Janvier & Boyett, 1996*a*). In the model, the Ca^{2+} transient is responsible for the initial peak. Repolarization is responsible for the second peak (the increase in the driving force on the exchanger as the membrane repolarizes more than compensates for the continuing decline in intracellular Ca^{2+}). Presumably, during the normal ferret ventricular action potential the second peak is not observed as the increase in driving force during repolarization is not sufficient to compensate for the fall in intracellular Ca^{2+} – in the case of the normal ferret ventricular action potential repolarization is occurring from a less positive potential.

In conclusion, during the ventricular action potential, even though the membrane potential is relatively positive, an inward current triggered by the Ca^{2+} transient, consistent with inward i_{NaCa}, makes a substantial contribution to the maintenance of the action potential plateau.

Bouchard, R. A., Clark, R. B. & Giles, W. R. (1993). Regulation of unloaded cell shortening by sarcolemmal sodium–calcium exchange in isolated rat ventricular myocytes. *Journal of Physiology* **469**, 583–599.

Boyett, M. R., Kirby, M. S. & Orchard, C. H. (1988). Rapid regulation of the 'second inward current' by intracellular calcium in isolated rat and ferret ventricular myocytes. *Journal of Physiology* **407**, 77–102.

Boyett, M. R., Moore, M., Jewell, B. R., Montgomery, R. A. P., Kirby, M. S. & Orchard, C. H. (1988). An improved apparatus for the optical recording of contraction of single heart cells. *Pflügers Archiv* **413**, 197–205.

Boyett, M. R., Deane, G. B., Newcombe, A. & Orchard, C. H. (1989). A versatile pulse generator for controlling physiological experiments. *Journal of Physiology* **416**, 2*P*.

Cannell, M. B. & Lederer, W. J. (1986). A novel experimental chamber for single-cell voltage-clamp and patch-clamp applications with low electrical noise and excellent temperature and flow control. *Pflügers Archiv* **406**, 536–539.

Cheng, H., Cannell, M. B. & Lederer, W. J. (1994). Propagation of excitation–contraction coupling into ventricular myocytes. *Pflügers Archiv* **428**, 415–517.

Egan, T. M., Noble, D., Noble, S. J., Powell, T., Spindler, A. J. & Twist, V. W. (1989). Sodium–calcium exchange during the action potential in guinea-pig ventricular cells. *Journal of Physiology* **411**, 639–661.

Ehara, T., Noma, A. & Ono, K. (1988). Calcium-activated non-selective cation channel in ventricular cells isolated from adult guinea-pig hearts. *Journal of Physiology* **403**, 117–133.

Grantham, C. J. & Cannell, M. B. (1995). Time course of calcium influx during the cardiac action potential recorded from isolated guinea-pig ventricular myocytes. *Journal of Physiology* **487.P**, 18–19*P*.

Hille, B. (1992). *Ionic Channels of Excitable Membranes*. Sinauer Associates, Sunderland, MA, USA.

Horackova, M., Beresewicz, A. & Isenberg, G. (1988). Effect of reduced Na gradient on electrical activity in isolated bovine and feline ventricular myocytes. *Canadian Journal of Physiology and Pharmacology* **66**, 222–232.

Janvier, N. C. & Boyett, M. R. (1996*a*). The role of Na^+–Ca^{2+} exchange current in the cardiac action potential. *Cardiovascular Research* **32**, 69–84.

Janvier, N. C. & Boyett, M. R. (1996*b*). The use of the action potential clamp technique to measure inward Na^+–Ca^{2+} exchange current during the action potential in isolated ferret ventricular myocytes. *Journal of Physiology* **491.P**, 155*P*.

Janvier, N. C. & Boyett, M. R. (1996*c*). Indirect regulation of the calcium current in ferret ventricular myocytes by the 4-AP sensitive transient outward current. *Biophysical Journal* **70**, 2, A56.

Janvier, N. C., Boyett, M. R. & Harrison, S. M. (1994). Control of action potential duration by Na^+–Ca^{2+} exchange current in ferret ventricular myocytes. *Journal of Physiology* **477.P**, 19–20*P*.

Kentish, J. C. & Boyett, M. R. (1983). A simple electronic circuit for monitoring changes in the duration of the action potential. *Pflügers Archiv* **398**, 233–235.

Kirshenlohr, H. L., Grace, A. A., Clarke, S. D., Shachar-Hill, Y., Metcalfe, J. C., Morris, P. G. & Smith, G. A. (1994). Calcium measurements with a new high-affinity n.m.r. indicator in the isolated perfused heart. *Biochemical Journal* **293**, 407–411.

Kiyosue, T., Spindler, A. J., Noble, S. J. & Noble, D. (1993). Background inward current in ventricular and atrial cells of the guinea-pig. *Proceedings of the Royal Society* B **252**, 65–74.

Lee, K. S., Marban, E. & Tsien, R. W. (1985). Inactivation of calcium channels in mammalian heart cells: joint dependence on membrane potential and intracellular calcium. *Journal of Physiology* **364**, 395–411.

LeGuennec, J.-Y. & Noble, D. (1994). Effects of rapid changes of external Na^+ concentration at different moments during the action potential in guinea-pig myocytes. *Journal of Physiology* **478**, 493–504.

Leitch, S. P. & Brown, H. F. (1996). Effect of raised extracellular calcium on characteristics of the guinea-pig ventricular action potential. *Journal of Molecular and Cellular Cardiology* **28**, 541–551.

Mitchell, M. R., Powell, T., Terrar, D. A. & Twist, V. W. (1984). The effects of ryanodine, EGTA and low-sodium on action potentials in rat and guinea-pig ventricular myocytes: evidence for two inward currents during the plateau. *British Journal of Pharmacology* **81**, 543–550.

Miura, Y. & Kimura, J. (1989). Sodium–calcium exchange current. Dependence on internal Ca and Na and competitive binding of external Na and Ca. *Journal of General Physiology* **93**, 1129–1145.

Noble, D. & Bett, G. (1993). Reconstructing the heart: a challenge for integrative physiology. *Cardiovascular Research* **27**, 1701–1712.

Noble, D., Noble, S. J., Bett, G. C. L., Earm, Y. E., Ho, W. K. & So, I. K. (1991). The role of sodium–calcium exchange during the cardiac action potential. *Annals of the New York Academy of Sciences* **639**, 334–353.

Spindler, A. J., Noble, S. J. & Noble, D. (1995). Gating and amplitude of guinea-pig ventricular i_{k1} is modified by extracellular Na^+. *Journal of Physiology* **487**, 133*P*.

Terrar, D. A. & White, E. (1989). Changes in cytosolic calcium monitored by inward currents during action potentials in guinea-pig ventricular cells. *Proceedings of the Royal Society* B **238**, 171–188.

Tohse, N. (1990). Calcium-sensitive delayed rectifier potassium current in guinea pig ventricular cells. *American Journal of Physiology* **258**, 1200–1207.

Vaughan-Jones, R. D., Lederer, W. J. & Eisner, D. A. (1983). Ca^{2+} ions can affect intacellular pH in mammalian cardiac muscle. *Nature* **301**, 522–524.

Zygmunt, A. C. & Gibbons, W. R. (1991). Calcium-activated chloride current in rabbit ventricular myocytes. *Circulation Research* **68**, 424–437.

Acknowledgements

This work was supported by a grant from the Wellcome Trust. N.C.J. is a Wellcome Prize student. We would like to thank Dr Munir Hussain for useful comments and help in isolating the cells and Luke Blumler, Andy O'Brien and Dave Johannson for excellent technical and photographic assistance.

Author's email address

M. R. Boyett: m.r.boyett@leeds.ac.uk

Received 14 March 1996; *accepted 30 July 1996.*